Temperature and pH influence on Diuron adsorption by Algerian Mont-Na Clay

Salima Tlemsani, Zoubida Taleb, Laurence Piraúlt-Roy, Safia Taleb

Temperature and pH influence on Diuron adsorption by Algerian Mont-Na Clay

Salima Tlemsani[a], Zoubida Taleb[a], Laurence Pirault-Roy[b] and Safia Taleb[a]

[a]Laboratory of Materials & Catalysis, Faculty of Exact Sciences, Djillali Liabes University, Sidi Bel-Abbes, Algeria;
[b]Institute of Chemistry of Poitiers: Materials and Natural Resources, UMR CNRS, University of Poitiers, Poitiers, France

ABSTRACT

The United States Environmental Protection Agency (EPA) classified the phenylurea herbicide Diuron ($C_9H_{10}Cl_2N_2O$) as possibly carcinogenic to humans. This research is focused on the adsorbent performances of an Algerian sodium Montmorillonite (Mont-Na), for the removal of Diuron in aqueous solutions. The material is characterized before and after processing using X-ray diffraction (XRD), Fourier transform infrared spectroscopy (FTIR), specific surface area (S_{BET}) and thermal analysis (TGA/DTA). The tests were firstly performed at25°C and pH = 6.3. Until 61 hours of experiment, no removal was obtained in this case. After that, the experiments were carried out onMont-Na at high temperature and medium pH (T = 45°C, pH = 6.3)and then at ambient temperature and basic pH (T = 25°C, pH = 11). The removal was increased from 74% to 91%, respectively. The equilibrium is reached after 5 hours and the adsorption capacity isbetween 0.74 mg/g at 45°C and 0.91 mg/g at pH = 11. The kinetic modelling shows that the pseudo-first order describes the experimental data of the Diuron adsorption on Mont-Na and the equili brium data are modelled perfectly by applying the Elovich model.The thermodynamic quantities indicate that the adsorption processon Mont-Na at pH = 6.3 is spontaneous ($\Delta G < 0$) and endothermic (ΔH = 31.80 kJ.mol^{-1}). In conclusion, under the operating conditionsused, local Mont-Na proved to be an excellent material for the adsorption of Diuron in aqueous solutions. That could be very promising for sewage treatment.

KEYWORDS

Diuron; adsorption; removal;Mont-Na; temperature; pH

1. Introduction

Water pollution is one of the greatest challenges humans faced in recent years. This is mainly due to the increase in human population and to technological and economic advances for the well-being of society such as the supply of medicines, plastics and batteries. The presence of non-biodegradable or persistent organic compounds (drugs, pesticides, and dyes), microparticles or heavy metals are found in water [1]. However, these compounds are sometimes toxic at very low doses, such as only a few ng/kg of body weight per day. Moreover, their persistent nature and bioaccumulative

aggravates the health problems [2].

In order to protect the environment and face environmental problems, researchers developed some techniques to eliminate these pollutants. Among them: ozonation [3], oxidation [4,5], coagulation [6], electrodegradation [7], etc. In addition, adsorption is among the oldest methods as an efficient, inexpensive and easy-to-implement technique [8], using different types of adsorbents: activated carbon [9], hydroxyapatite [10] or bentonite [3,11,12]. These last are interlayer aluminosilicates minerals with different structures, such smectite. Bentonites are abundant and made up primarily of Montmorillonite. Application of Montmorillonites was previously used for adsorption of o-cresol [3,11]. They have been chosen because of their thermal stability, their low cost and high adsorption capacity [5,12].

Conventionally, herbicides applied on excess causing serious problems in fact during their application, they can lead to the loss of biodiversity. Intensive farming operations could potentially contaminate groundwater with a variety of pesticides [13]. Thus, today in tap water some pesticides such as Atrazine and Diuron are always identified. Diuron is a substituted urea herbicide that has been widely used since the 1950s to control broadleaf weeds and herbaceous annuals and perennials, as well as mosses. The presence of Diuron in water poses a serious risk to human health, soil and ecosystems aquatic as well as the environment because it is a CMR product, carcinogenic to category 3 [14]. Although banned since 2008, the persistence of Diuron is such that, like Atrazine, it will take more than 50 years to eliminate. Over the course of several years, materials have been tested for the adsorption of Diuron including aluminosilicate minerals and carbon-based materials [15,16]. For example, the multi-walled carbon nanotubes (MWCNTs), the study helps to understand that their adsorption capacity is greater than that of sepiolite, and ash [17].

The authors are interested in the adsorbent characteristics of a local Montmorillonite, which attracts the attention of many researchers, taking into account its environmental, societal and economic importance. In order to a better knowledge of the adsorption of Diuron, a series of experiments has been adopted. Two processes of Diuron adsorption were highlighted on: Mont-Na at 45°C in neutral medium; Mont-Na at 25°C in basic medium (pH = 11). The optimal adsorption conditions were determined, applying kinetics, adsorption isotherms and thermodynamic studies. The surface of the material has been also characterised. All the graphics in this work were created using Origin 2018 program.

2. Research methodology

2.1. Montmorillonite-Na (Mont-Na) and adsorbate

The clay chosen for this research was sodium Montmorillonite (Mont-Na) obtained from an Algerian company (National Company of Non-Ferrous Mining Products, ENOF).

Diuron (98%) was purchased from Sigma Aldrich (Poitiers, France) and used as pollutant. The aqueous solution of Diuron at different concentrations was covered with aluminium foil and was prepared in darkness, by dissolving a required proportion of the Diuron in distilled water, under heating without reaching the boiling temperature of Diuron (180°C). The λmax was determined at 248 nm using UV–Vis analysis.

2.2. Analytical methods

To identify the bands that characterise the normal modes of vibration and the remarkable functional groups present in Mont-Na, Fourier transform infrared spectro- scopy was performed (Perkin Elmer FTIR Spectrometer Frontier, Algeria). The interlayer distance dhkl of the materials was detected by X-ray diffraction (XRD) (EMPYREAN PANalytical diffractometer, France) operated at the Kα copper wavelength (λ = 1.5406) and coupled with an Xcelerator linear detector. The specific surface (SBET) of Mont-Na was estimated using the Brunauer, Emett and Teller (BET) method. The textural measurements were realised using a volumetric adsorption device (Micromeritics Smart VacPrep type, France). The SBET surface area was calculated by the nitrogen gas adsorption/desorption isotherms at 77 K under standard pressure conditions. The thermal analysis (TGA/DTA) was carried out under argon in a temperature range of 20– 500°C with a heating rate of 20°C/min. This was done using a thermal analysis device (SDT Q66 V8.3, France).

In the other hand, solutions were analysed by UV–Visible spectrophotometer (Perkin Elmer-Lambda 45 type). pH was measured with an Advanced Water Quality Sensor PS- 2230. To obtain cleaner samples and for eliminating interference caused by clay, a 'Centrifugal-Apagee Swing 3000' centrifuge was using in addition to the syringe filters (0.45 µm).

2.3. Batch adsorption

First, the influence of different physicochemical parameters on Diuron-Mont-Na interactions (time, initial solute concentration, pH, temperature) was studied. For each experi- ment, the clay was brought into contact with distilled water, where the Diuron has been dissolved. Identical solution volumes (50 mL) with 1 g of Mont-Na were treated.

In the second experiments, the influence of these parameters (time, initial concentra- tion of the solute) was studied at basic pH (pH = 11), while keeping the same operating conditions above. After a predetermined time, the samples were centrifuged for 15 min- utes and then filtered by a syringe filter. Percent removal, adsorption capacity at time t qt (mg/g) and adsorption capacity at equilibrium qe (mg/g) were calculated according to the following equations (Equation (1), (2) and (3), respectively) [3]:

$$\%\text{removal} = [\,(C_0 - C_e) / C_0\,] \times 100 \qquad (1)$$

$$q_e = [\,(C_0 - C_t) / W\,] \times V \qquad (2)$$

$$q_e = [\,(C_0 - C_e) / W\,] \times V \qquad (3)$$

Where, C_0 and C_e (mg/L) are the initial and equilibrium Diuron concentrations, respectively; V (L) is volume of the solution and W (g) is the mass of adsorbent (Mont-Na).

2.3.1. Time and temperature effect on Diuron adsorption

The influence of the time on the elimination of Diuron on the used material was examined in two sets of experiments: Introduction of 1 g of Mont-Na in 50 mL of Diuron solution (20 mg/L), at the medium pH (pH = 6.3). The manipulations were performed at room temperature (25°C), varying the stirring time from 0 to 61 hours. Then, the experiments were performed during 6 hours at 45°C using a reflux heating assembly that allows the conduct of the reaction at constant temperature and without loss of materials. The handling ends when the equilibrium was reached.

In order to examine the behaviour of the material with Diuron when its concentration is modified during the two adsorption processes, six different initial concentrations have been chosen of: 15, 20, 25, 30, 35 and 40 mg/L. This choice is limited by the Diuron solubility.

2.3.2. Effects of pH on Diuron adsorption

To study the influence of pH on adsorption of Diuron on Mont-Na; in first 1 g of Mont-Na was introduced in 50 mL of Diuron solution (20 mg/L) maintained at stirring time of 6 hours, at room temperature (25°C). Before adding Mont-Na, the pH was adjusted with HCl (0.1 M) and NaOH (0.1 M) solutions and varied from 2 to 11.

2.3.3. Kinetics adsorption

In the aim to determine the retention kinetics order of Diuron with Mont-Na, three kinetic models have been tested: 1) pseudo-first-order (Equation (4)); 2) pseudo-second-order (Equation (5)) and 3) Elovich (Equation (6)), as follows [3]:

$$\ln (q_e - q_t) = \ln q_e - k_1 t \quad (4)$$

$$1/(q_e - q_t) = 1/q_e + k_2 t \quad (5)$$

$$q_t = [\ln(\alpha_E . \beta_E)]/\beta_E + (1/\beta_E) . \ln t \quad (6)$$

Where, K_1 (min^{-1}) is Pseudo-first-order kinetic constant and K_2 represents Pseudo-second- order kinetic constant. β_E ($g.mg^{-1}$) parameter related to the extent of surface coverage and activation energy. α_E (mg/ g.min) represents initial adsorption rate.

2.3.4. Adsorption isotherm

Adsorption isotherms have an important role in the determination of adsorbent capacity. The obtained results of the influence of the initial Diuron concentration during the study were used to draw them. There are many theoretical models that have been developed to describe adsorption isotherms. However, the models of Langmuir, Freundlich, Elovich and Temkin were chosen.

The exploitation of the formula $q_e = f(C_e)$ in its linear form of Freundlich (Equation (7)) and also that of Langmuir (Equation (8)), Elovich (Equation (9)) and Temkin (Equation (10)) allowed to deduce the main parameters characterizing each model as shown below [3]:

$$\log q_e = \log (k_F) + n \log C_e \quad (7)$$

$$1/q_e = 1/(C_e q_m K_L) + 1/q_m \quad (8)$$

$$\text{Ln } (q_e/C_e) = \ln (q_m K_E) - (q_e/q_m) \quad (9)$$

$$q_e = B_T \ln k_T + B_T \ln C_e \quad (10)$$

With; K_F (mg/L) and n are Freundlich constants related to the adsorption capacity and adsorption intensity, respectively. K_L: Langmuir constant (L/mg). q_m: theoretical maximum adsorption capacity (mg/g). K_E: Elovich constant (L/mg). R: universal gas constant (8.314 J/mol.K). T: Temperature (K). K_T: Temkin constant (L/mg). B_T: related to the activation energy (J/mol)

2.3.5. Temperature effect and thermodynamic properties

Thermodynamic properties such as enthalpy, entropy and free energy (Gibbs) are essential for the study of any adsorption system. These properties determine the nature of adsorption and spontaneity. Thermodynamic relationships (Equations 11, 12) were used to determine the standard enthalpy change (ΔH), standard entropy change (ΔS) and standard Gibbs free energy change (ΔG) [18]::With; KF (mg/L) and n are Freundlich constants related to the adsorption capacity and adsorption intensity, respectively. KL: Langmuir constant (L/mg). qm: theoretical max- imum adsorption capacity (mg/g). KE: Elovich constant (L/mg). R: universal gas constant (8.314 J/mol.K). T: Temperature (K). KT: Temkin constant (L/mg). BT: related to the activation energy (J/mol).

2.3.5. Temperature effect and thermodynamic properties

Thermodynamic properties such as enthalpy, entropy and free energy (Gibbs) are essential for the study of any adsorption system. These properties determine the nature of adsorption and spontaneity. Thermodynamic relationships (Equations 11, 12) were used to determine the standard enthalpy change (ΔH), standard entropy change (ΔS) and standard Gibbs free energy change (ΔG) [18]:

$$\text{Ln } K_p = - \Delta H/RT + \Delta S/R \quad (11)$$

$$\Delta G = - RT \ln K_p \quad (12)$$

Where, K_P is the thermodynamic equilibrium constant and it is the ratio of concentration of adsorbate in the solid and liquid phases. ΔH and ΔS were derived from the slope and intercept of the linear plot (i.e. Van't Hoff plot) of lnKp versus 1/T, respectively.

Adsorption experiments were carried out at four different temperatures (25°C, 45°C, 60°C and 80°C)

3. Results and discussion

3.1. Adsorbent characterisation before Diuron adsorption

3.1.1. FTIR analysis

The FTIR spectrum of Mont-Na is shown in Figure 1. The spectrum of Mont-Na represents two absorption bands characterising the OH bonds, located between 3800 and 3200 cm−1 with central bands at 3622 cm−1 and at 3400 cm−1 [19], characteristic of Montmorillonites. The small band at 1635 cm−1 is attributed to the valence vibrations (stretching) of the OH bond of water constitution and to the vibrations of bending of the bonds of water molecules adsorbed between the sheets. The recorded spectrum represents an absorp- tion band centred at around of 1005 cm−1 attributed to Si-O bond stretching vibrations.

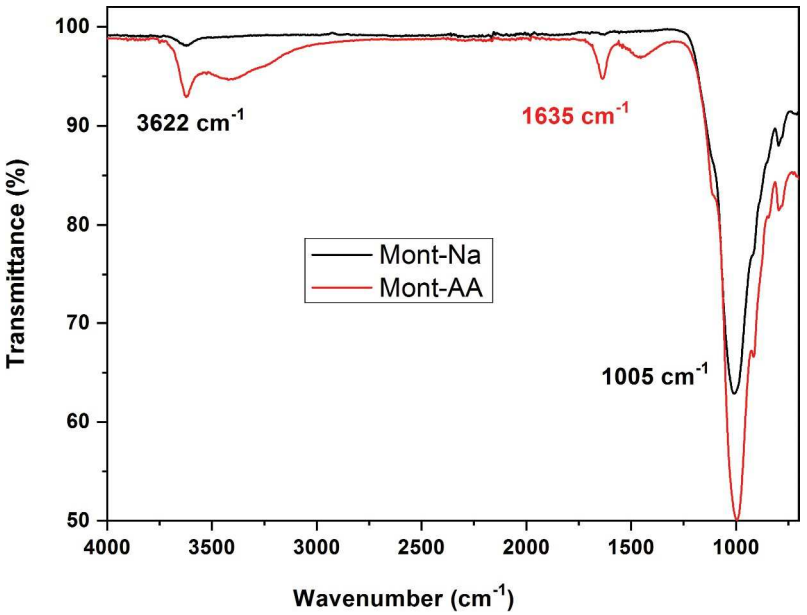

Figure 1. The FTIR spectra of Mont-Na and Mont-AA.

3.1.2. X- ray diffraction (XRD)

The predominant peaks seen on the Mont-Na diffractogram in Figure 2 are those of; silica SiO2 α-quartz (2θ = 27°), Montmorillonite (2θ = 17.5°). In addition, a characteristic peak of illite (2θ = 9°) is observed [14]. The examination of the spectrum mainly shows an intense line (below 2θ = 10°, line between 15° and 30°) of X-ray diffractions, specific to Montmorillonite [13]. Previously, the diffractogram examination of local clay (Mont-Na) also indicates a basal spacing of 12.6 Å [4].

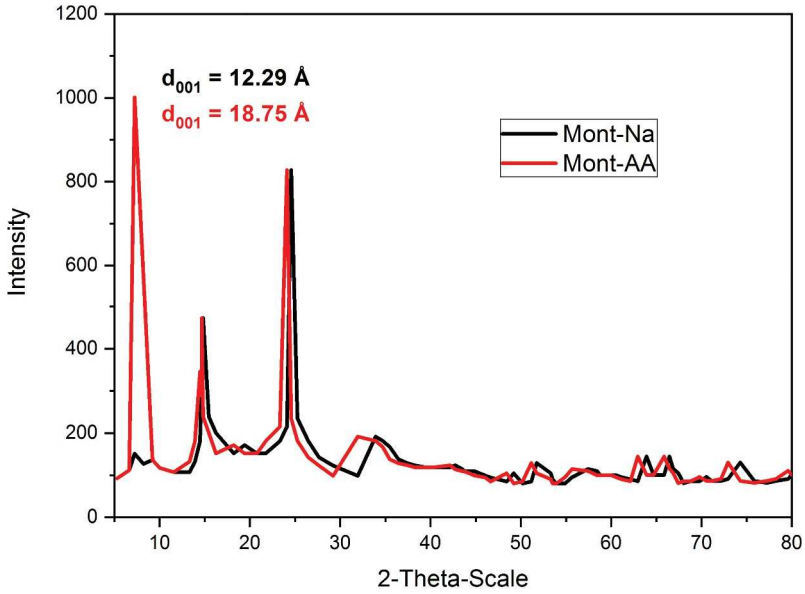

Figure 2. X- Ray Diffractogram of Mont-Na and Mont-AA.

Table 1. BET-specific surface area values of Mont- Na and Mont- AA.

Sample	Mont-Na	Mont-AA
S_{BET} (m^2/g)	43	65
Volume of micropores (cm^3/g)	0.007	0.016
Pore diameter (Å)	69	51

3.1.3. BET surface area (SBET)

It should be noted that BET equation is generally applicable only over a certain range of relative pressures (between 0.05 and 0.35), where theoretical and practical curves agree. As it is shown in Table 1.

3.1.4. Thermogravimetric analysis

In Figure 3, for TGA of Mont-Na two levels were noticed: an endothermic peak at 90°C, associated with a weight loss of about 1.8%. The latter is linked to the elimination of the water physisorbed at the surface of the particles. The strong intensity of the first peak confirms the presence of a rising phase (smectite) interbedded with non-swelling clay [20]. A second endothermic peak around 450°C accompanied by a weight loss of about 2.3%, this peak corresponds to the water adsorbed in the interfoliar space. The absence of the 'shoulder' which normally appears close to the endothermic peak of 90°C in the DTA curve in the case of Montmorillonite has proved that this martial is of the sodium type. This is consistent with the X-ray diffraction data as well. The adsorption capacity of clay is directly proportional to the amount of water adsorbed on

the clay surface, represented by the first endothermic peak at 90°C.

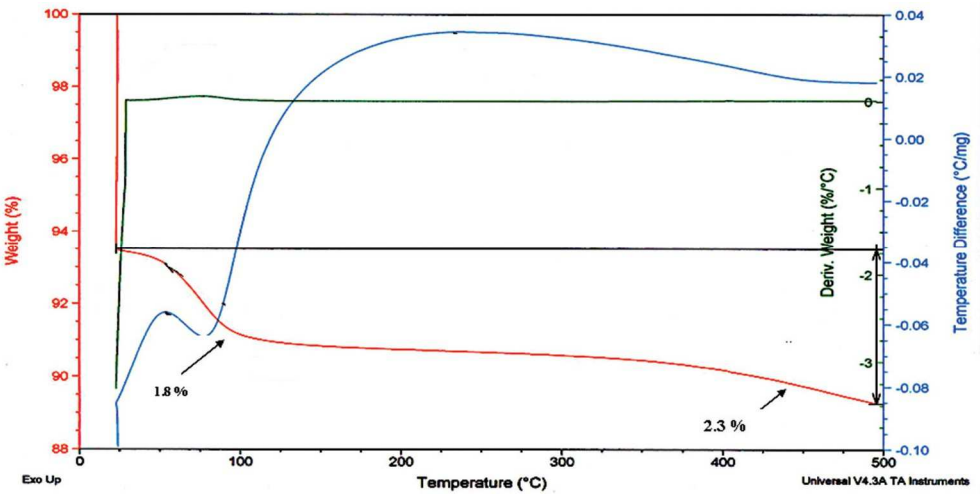

Figure 3. Thermogravimetric analysis of Mont- Na.

3.2. Adsorption studies

3.2.1. Effect of contact time and temperature

The decrease in absorbance was not achieved during a contact time of 61 hours at 25°C, which precludes determination of adsorbed quantities and the retention of Diuron (20 mg/L) on Mont-Na is therefore impossible at room temperature. In an attempt to solve this problem, temperature was increased to T = 45°C, for the first time. In this case, the shape of the curve (Figure 4(a)) shows that equilibrium is reached at only 5 hours with an adsorption capacity of 0.74 mg/g on 1 g Mont-Na. It is therefore conceivable that temperature at 45°C promotes the adsorption kinetics of Diuron on Mont-Na, with minimising the contact time and achieving a good removal.

3.2.2. Effect of pH

In the second time, temperature was maintained at 25°C, but pH was modified from 2 to 11 during 5 hours experiments. The obtained results regrouped in Figure 5 shows that the best pH for Diuron adsorption on Mont-Na was a basic pH (pH = 11).

Examination of the influence of this parameter on the adsorption of Diuron clearly indicates that pH plays an important role. It can be seen that the passage to the basic medium (pH = 11) leads to a considerable increase in the removal and retention efficiency of Mont-Na. It increased from 73% in acid medium (pH = 2) to 91% in basic medium (pH = 11). This prompted us to optimise the parameters of Diuron adsorption on Mont-Na at pH = 11 and the results were favourable without needing to increase the temperature.

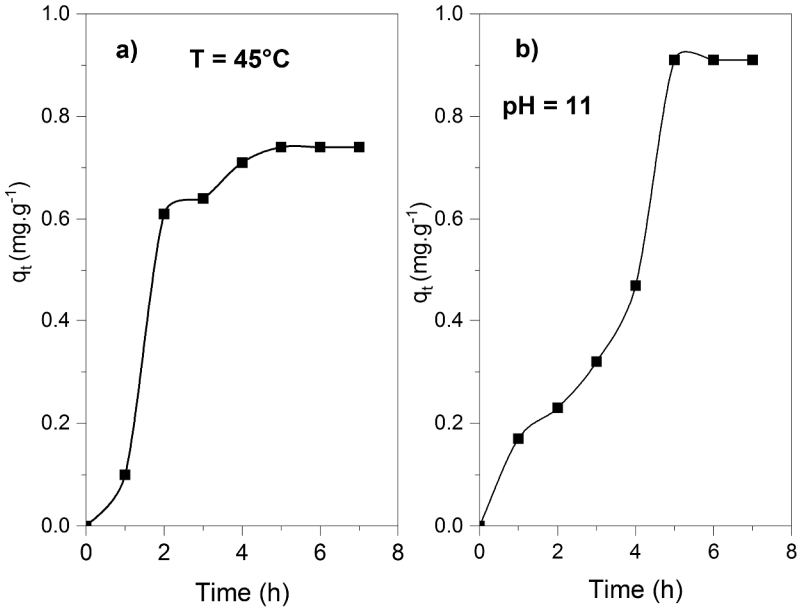

Figure 4. Effect of contact time on the removal of Diuron (20 mg/L) on Mont-Na ($m_{adsorbent}$ = 1 g. V = 50 mL) (a) T = 45°C, pH = 6.3 and (b) pH = 11, T = 25°C.

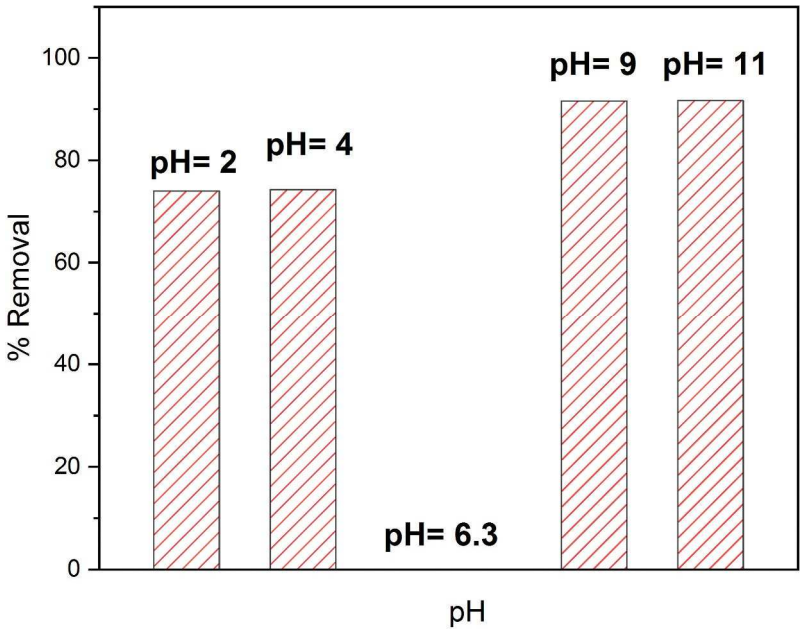

Figure 5. Effect of pH on removal of Diuron (20 mg/L) on Mont-Na (t = 5 h, T = 25°C, $m_{adsorbent}$ = 1 g, V = 50 mL).

This would be explained by the fact that; hydroxyl groups are however pH dependent: At low pH, the surface hydroxyls are fully protonated (OH), the clay shows a generally positive border charge. At high pH, the hydroxyls deprotonate, the surface is globally

negative (O2-). The variable loads are much less important than the permanent loads, but still play a role in the clay exchange capacity. On the other hand, the Diuron molecules (C9H10Cl2N2O) have strongly negative polar regions corresponding to pairs of the oxygen atom, as well as very positive polar hydrogen atoms around N-H group. Therefore, oxygen and N-H groups can be considered as acceptors and hydrogen bond donors. While, the best adsorption of Diuron on HTC @ ANS-200 occurred at a pH value close to the value of (7.3) [17].

At pH = 11, the amount of adsorption increases until the time balance of the adsorbent of 5 h and adsorption capacity of 0.74 mg/g on 1 g Mont-Na (Figure 4(b)). A desorption phenomenon could be observed after this time of 5 h, demonstrating the exchange reversibility involved.

The continuation of our study will be carried out in the same last experiment conditions: T = 45°C and medium pH then T = 25°C and basic pH (pH = 11).

3.2.3. Effects of initial adsorbate concentration

It is noted that Mont-Na adsorbs a maximum amount of Diuron at a concentration of 20 mg/L at T = 45°C (Figure 6(a)). The results can be explained, which indicates that at this concentration the substrate has numerous available specific sites and adsorbs better. On the other hand, the retention increases slightly to 30 mg/L after a clearly obvious decrease, so that it becomes stable thereafter, since all the clay sites are occupied or difficult to access. However, it is found that the competition for the specific adsorption by Mont-Na is not important with the increase of the initial concentration of Diuron.

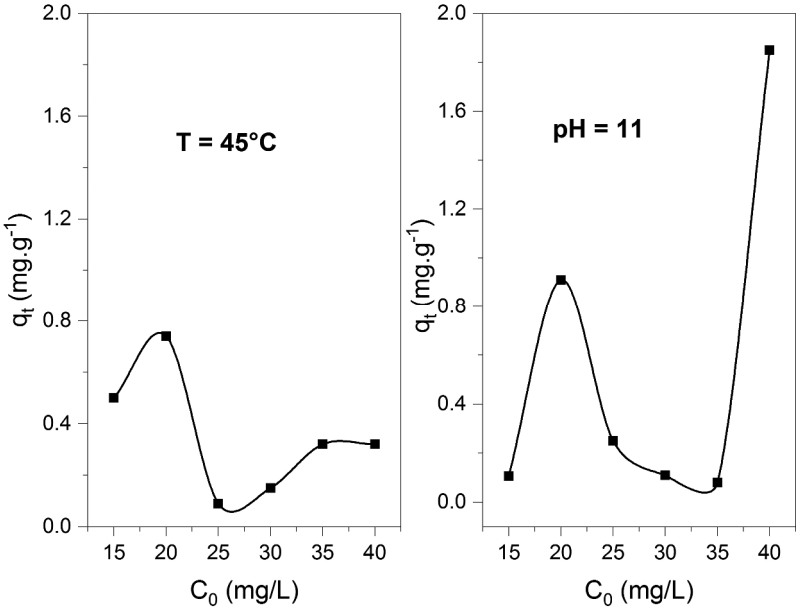

Figure 6. Effect of initial concentration of Diuron (mg/L) on adsorption capacity qe on Mont-Na during t = 5 h, $m_{adsorbent}$ = 1 g, V = 50 mL: (a) T = 45°C, pH = 6.3 and (b) p H = 11, T = 25°C.

At pH = 11 (Figure 6(b)), it is almost difficult to obtain the optimal reliable concentration, and the retention of Diuron on Mont-Na increases obviously for a concentration of 40 mg/L.

3.3. Adsorption kinetic modelling

Adsorption Diuron kinetics on Mont-Na was studied by fitting experimental data to pseudo-first order (Figure 7), pseudo-second order (Figure 8) and Elovich kinetic models (Figure 9). As it can be observed from the obtained parameters, the experimental adsorbed quantity (qe expt) and correlation coefficients calculated from the equations cited previously (see section 2.2.3) and regrouped in Table 2, it can be concluded that the adsorption processes cannot be expressed by the pseudo-second-order, because the negative values of the calculated quantities ($q_e$cal) have no physical meaning. However, the retention of Diuron on Mont-Na is well described by pseudo-first-order kinetic (R2 = 0.948) and the retention of Diuron on Mont-Na at basic pH is well modelled by the Elovish model (R2 = 0 .999). While the removal of the herbicide Diuron on the granulated Basassu coconout activated charcoal was best described through pseudo first-order model [21].

3.4. Adsorption isotherm modelling

From the values obtained from Freundlich isotherm (Figure 10), Langumir isotherm (Figure 11), Elovich isotherm (Figure 12) and Temkin isotherm (Figure 13) reported in the Table 3 for the correlation factors R2, the retention of Diuron by both Mont-Na, followed the Elovich adsorption isotherm (R2 = 0.965). This reflects a kinetic development assuming that adsorption sites increase exponentially with adsorption, which implies multilayer adsorption. While, the equilibrium data were well-adjusted to the Langmuir isothermal model, indicating probably monolayer biosorption of Diuron on Anabaena sphaerica and Scenedesmus obliquus [22].

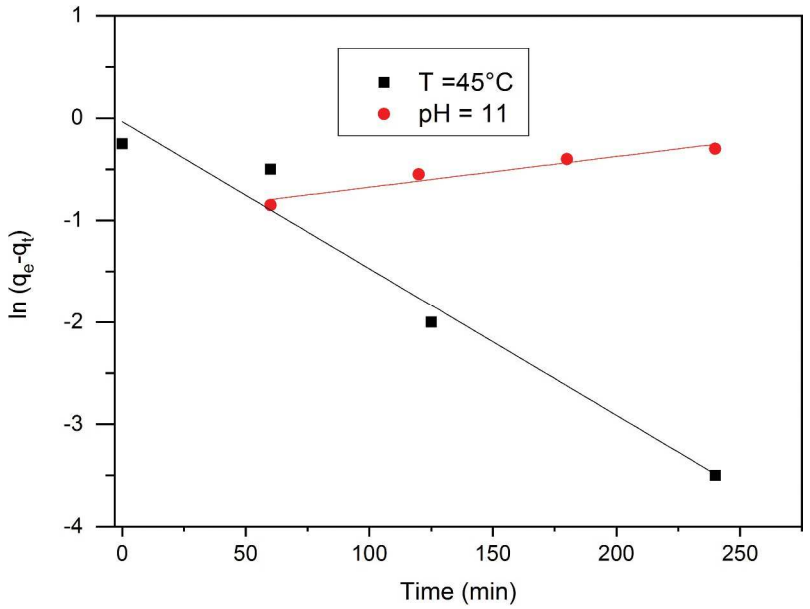

Figure 7. Pseudo-first order model of Diuron adsorption on Mont-Na.

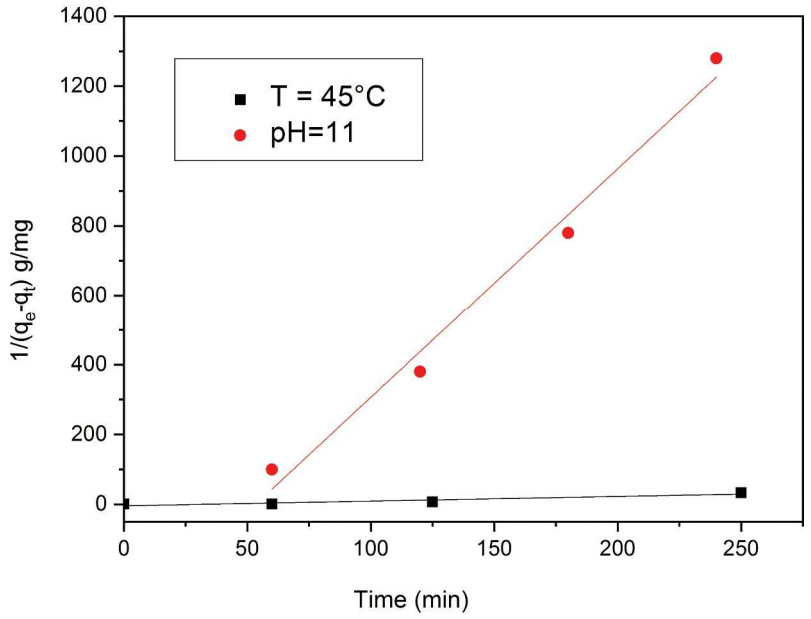

Figure 8. Pseudo-second order model of Diuron adsorption on Mont-Na.

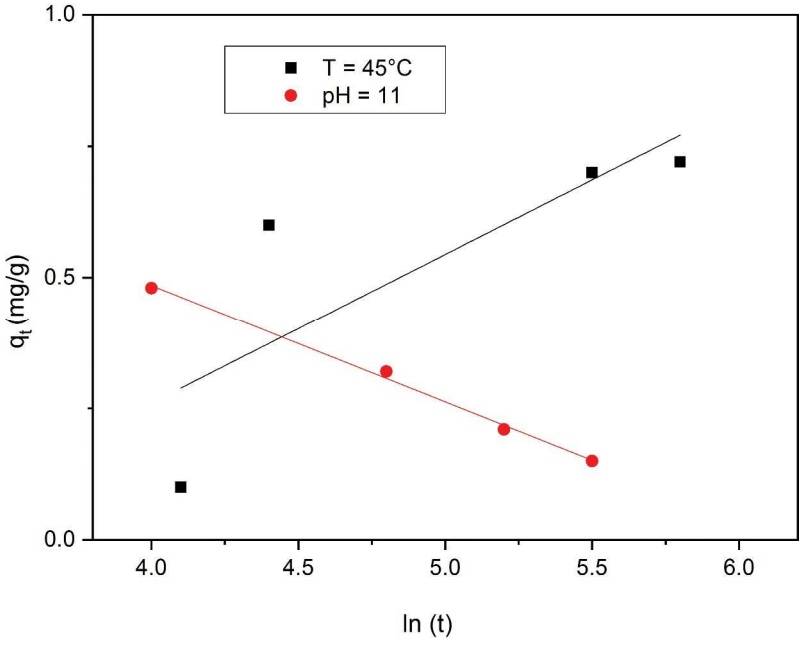

Figure 9. Elovich kinetic model of Diuron adsorption on Mont-Na.

Table 2. Parameters and correlation coefficients for different adsorption kinetic models applied to experimental data of Diuron adsorption on Mont-Na.

	Adsorption on Mont-Na at 45°C in neutral medium	Adsorption on Mont-Na at 25°C in basic medium
Kinetic models	q_e expt (mg/g) = 0.74	q_e expt (mg/g) = 0.91
Pseudo-first order	K_1 (min^{-1}) = - 0.014 q cal (mg/g) = 0.97 R^2 = 0.948	K_1 (min^{-1}) = 0.0029 q cal (mg/g) = 0.37 R^2 = 0.927
Pseudo-second order	K_2 (g/mg.min) = 0.139 q cal (mg/g) = - 0.27 R^2 = 0.889	K_2 (g /mg.min) = 6.56 q cal (mg/g) = - 0.003 R^2 = 0.963
Elovich	α_E (mg /g.min) = 0.01 β_E (g/mg) = 3.56 R^2 = 0.862	α_E(mg/g.min) = 4.4×10^{-4} β_E (g/mg) = - 4.54 R^2 = 0 .999

3.5. Thermodynamic study on Diuron adsorption in neutral pH

Thermodynamic analysis was studied only at neutral pH. At basic pH the results are already favourable and it is always preferable to modify only one parameter during the optimisation. The elimination of Diuron on Mont-Na stops above 45°C. Changes in standard thermodynamic properties were evaluated for Diuron (20 mg/L) adsorbed on Mont-Na, using the Van't Hoff diagram (Figure 14). The standard enthalpy (ΔH), standard entropy (ΔS) and standard Gibbs free energy (ΔG) values were calculated and shown in Table 4. Negative values of ΔG at different temperatures indicate the feasibility and spontaneity of the adsorption process. ΔG values between 0 and – 20 kJ/mol have been assigned for the physisorption process. The decrease in ΔG values with increasing temperature indicates that the adsorption is disproportionate to temperature. The positive value of ΔS (0.104 KJ/K.mol) represents the increase in randomness at the interphase of the solid solution during adsorption. The positive value of ΔH (31.80 kJ.mol-1) suggests that the process is endothermic, which means that the adsorption reaction consumes energy [23].

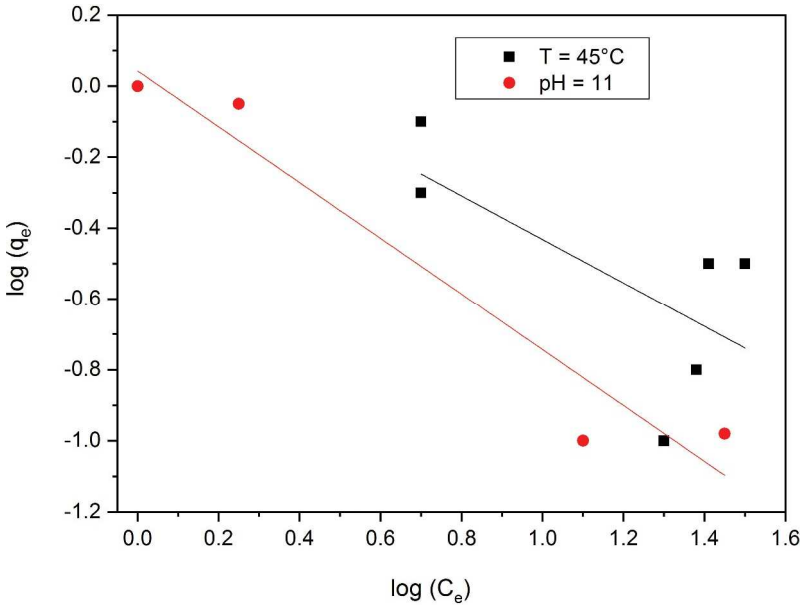

Figure 10. Freundlich adsorption isotherm of Diuron adsorption on Mont-Na.

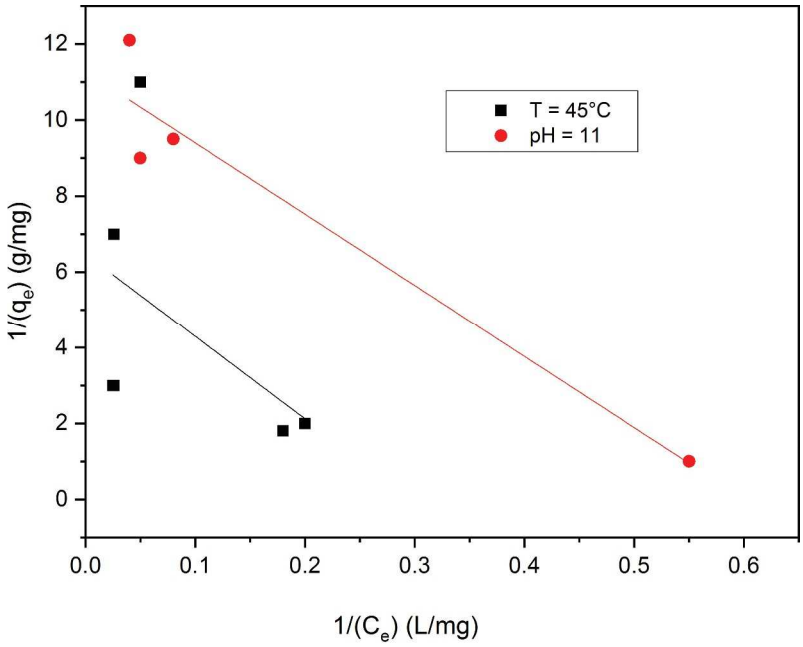

Figure 11. Langmuir adsorption isotherm of Diuron adsorption on Mont-Na.

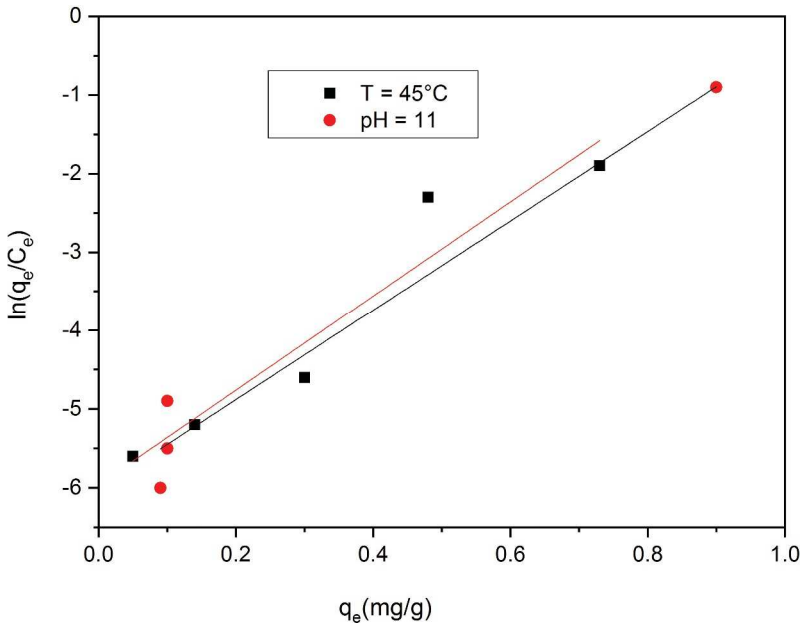

Figure 12. Elovich adsorption isotherm of Diuron adsorption on Mont-Na.

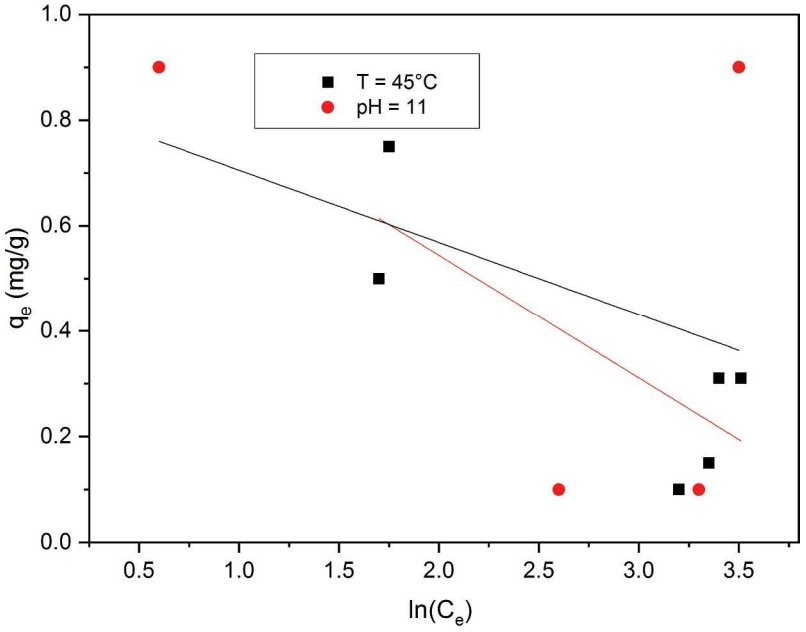

Figure 13. Temkin adsorption isotherm of Diuron adsorption on Mont-Na.

3.6. Adsorbent characterisation after Diuron adsorption experiments

It is important to indicate that the characterisation results of Mont-Na after the adsorption of Diuron are similar whether at neutral or basic pH and the pH did not influence the introduction of Diuron into the clay.

Table 3. Parameters and correlation coefficients for different adsorption isotherms models applied to experimental data of Diuron adsorption on Mont-Na.

Isotherm	Adsorption on Mont-Na at 45°C in neutral medium q_e expt (mg/g) = 0.74	Adsorption on Mont-Na at 25°C in basic medium q_e expt (mg/g) = 0.91
Freundlich	K_F [(mg/g)/(mg/L) 1/n] = 0.70 n = – 0.61 R^2 = 0.463	K_F [(mg/g)/(mg/l)1/n] = 1.09 n = – 0.7 R^2 = 0.933
Langmuir	q_{max} (mg/g) = 0.15 K_L (L/mg) = – 0.3 R^2 = 0.302	q_{max} (mg/g) = 0.089 K_L(L /mg) = – 0.59 R^2 = 0.919
Elovich	K_E (L/mg) = 3.3×10^{-4} q_m(mg/g) = 0.16 R^2 = 0.911	K_E (L/mg) = 2.05 q_m(mg/g) = 0.17 R^2 = 0.965
Temkin	K_T (L/mg) = 0.01 b_T (J/mol) = – 0.23 R^2 = 0.655	K_T (L/mg) = 0.001 b_T (J/mol) = – 0.13 R^2 = 0.914

3.6.1. FTIR analysis

The FTIR spectrum of Mont-Na after the adsorption of Diuron in Figure 1 shows that the characteristic bands at stretching bending vibrations of the different groups of Diuron are attributed as; NH (3300 cm−1), C = O (1650 cm−1), C-N (1299 cm−1) and the aromatic group (750 cm−1). Therefore, the pollutant is retained on Mont-Na.

3.6.2. X- ray diffraction (XRD)

In the Mont-AA diffractogram (Figure 2), an increase in d001 was observed; it goes from 12.61 to 18.75 Å. This variation is probably due to the presence of Diuron molecules incorporated in the interfoliar space during adsorption.

3.6.3. BET surface area (SBET)

The specific surface area of Mont-Na increased from 43.03 m2/g to 58.23 m2/g after the adsorption of Diuron (Table 1). The volume of the micropores has also increased, which is probably explained by the retention of the pollutant on the surface of this material.

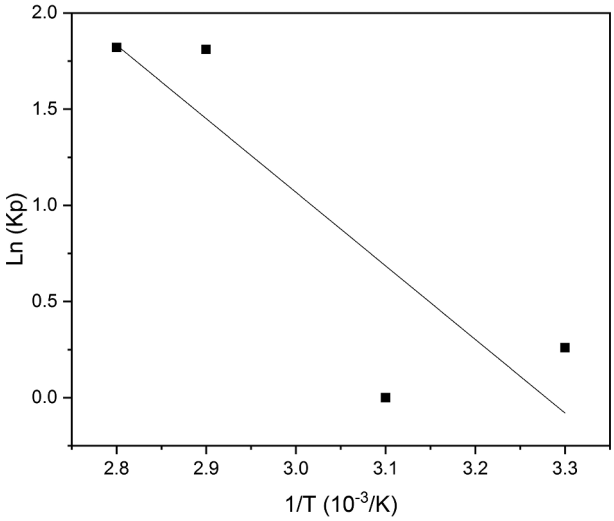

Figure 14. Van't Hoff diagram for Diuron adsorption on Mont-Na.

Table 4. Thermodynamic parameters of Diuron adsorption on Mont-Na at neutral pH.

Thermodynamic parameters				
ΔH (kJ.mol^{-1})	31.804			
ΔS (KJ/.K.mol)	0.104			
T (K)	298	318	338	353
ΔG (kJ.mol^{-1})	– 0.64	0	– 5.088	- 5.343

3.6.4. Thermogravimetric analysis

The curves of the TGA/DTA analysis of Mont-Na after adsorption are shown in Figure 15. The thermogravimetric evolution of the Diuron treatment includes two endothermic stages corresponding to the loss of the two different types of water discussed previously, and a third located around 150°C, relative to the melting temperature of Diuron (158.5°C). The weight loss is 3% for Mont-AA. This loss of mass produced by the increase in temperature is attributed to the desorption of surface water and/or structure formed due to the presence of Diuron.

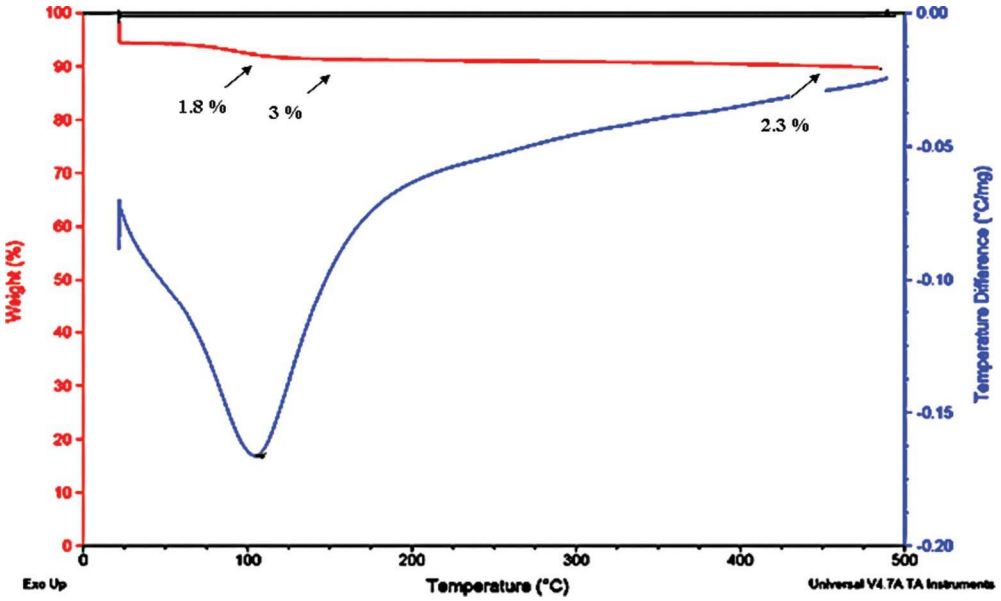

Figure 15. Thermogravimetric analysis of Mont-AA sample.

4. Conclusion

The results confirm the effectiveness and the usefulness of local Algerian Montmorillonite clay in the removal of Diuron from polluted waters.

The increase in temperature (T = 45°C and pH = 6.3) in a first case and pH (T = 25°C and pH = 11) in a second case made it possible to improve the percentage of Diuron removal with reducing the contact time. The equilibrium is reached at 5 hours instead of 61 hours without modification of operating conditions (neutral pH and ambient temperature).

The temperature at 45°C promotes the adsorption kinetics of Diuron on Mont-Na, with achieving a good removal. The passage to the basic medium (pH = 11) leads to an increase in the removal from 74% to 91% during adsorption, respectively. The retention of Diuron on Mont-Na is very well described by pseudo-first-order and the retention of Diuron on Mont-Na at pH = 11 is described by the Elovich model.

The two adsorption processes follow the Elovich isotherm, which implies multilayer adsorption. The negative ΔG values at different temperatures indicate the feasibility and spontaneity of the adsorption process, and the positive value of ΔH suggests that the process is endothermic. In conclusion, the use of the adsorbent properties of clay materials for the elimination of a herbicide and the improvement of the quality of water intended for human consumption seems to be an interesting solution and the improvement of water quality.

On the other hand, a mixture of the clay with other adsorbents could have a higher capacity compared to the clay alone. Taking into account the different techniques (photocatalysis, ozonation, etc.) and the advantages of adsorption, it is necessary to

study the combination of treatment technologies in an integrated system in order to eliminate the pollutants.

Acknowledgments

The Algerian Directorate General of Scientific Research and Technological Development (DGRSDT), and the Algerian Ministry of Higher Education and Scientific Research (MESRS) are greatly thanked for their financial support, even for making it possible to join the Algerian-French doctoral scholar- ships program: PROFAS B + 2019-2020, in order to accomplish and innovate this research work. The authors would like to thank the collaboration of the Institute of Chemistry of Poitiers (IC2MP) for having facilitated the analysis and characterization techniques.

References

[1] A.H. Bhat, T.A.R. Inamuddin and H.T.N. Chisti, Curr. Anal. Chem 18 (3), 269 (2020). doi:10.2174/ 1573411016999200729123309.

[2] K. Al-Akeel, InTech. (2017) [Online]. doi: 10.5772/intechopen.72776

[3] Z. Taleb, A. Ramdani, R. Berenguer, N. Ramdani, M. Adjir, S. Taleb, E. Morallón, S. Nemmich and A. Tilmatine, Int. J. Environ. Anal. Chem 2021. doi:10.1080/03067319.2020.1865335

[4] H. Herbache, A. Ramdani, Z. Taleb, R. Ruiz-Rosas, S. Taleb, E. Morallón, L. Pirault-Roy and N. Ghaffour, Water Environ. Res 91, 165 (2019). doi:10.1002/wer.1022.

[5] S. Tlemsani, Z. Taleb, L. Pirault-Roy and S. Taleb, Clean – Soil, Air, Water 50 (2) (2021). doi:10.1002/clen.202000468.

[6] A. Belbali, A. Benghalem, K. Gouttal and S. Taleb, Int. J. Environ. Anal. Chem 2021. doi:10.1080/ 03067319.2021.1995725

[7] Z. Taleb, F. Montilla, C. Quijada, E. Morallon and S. Taleb, Electrocatal 5, 186 (2014). doi:10.1007/s12678-013-0182-x.

[8] I. Bekri, Z. Taleb, S. Taleb, S. Tlemsani, G. Hodaifa and B. Abdelkader, Wastewater. Environ Qual Manage 2021. doi:10.1002/tqem.21823

[9] L. Qiu, Z. Dong, H. Sun, H. Li and C.C. Chang, Water Environ. Res. 88, 1855 (2016). doi:10.2175/ 106143016x14696400495811.

[10] A. Ramdani, S. Taleb, A. Benghalem, A. Deratani and N. Ghaffour, Desalin. Water Treat 54, 3444 (2015). doi:10.1080/19443994.2014.910838.

[11] A. Serouri, Z. Taleb, A. Mannu, S. Garroni, N. Senes, S. Taleb, S. Brini and S.K. Abdoun, Recycling 6 (68), 1 (2021). doi:10.3390/recycling6040068.

[12] H. Herbache, A. Ramdani, A. Maghni, Z. Taleb, S. Taleb, E. Morallon and B. Rachid, Desalin. Water Treat 57, 20511 (2016). doi:10.1080/19443994.2015.1108240.

[13] M. Chauhan, V.K. Saini and S. Suthar, J. Porous Mater 27, 383 (2020). doi:10.1007/s10934-019- 00817-8.

[14] S. Kurwadkar, Water Environ. Res. 91 (10), 1001 (2019). doi:10.1002/wer.1166.

[15] J. Liu, E. Morales-Narváez, T. Vicent, A. Merkoçi and G.H. Zhong, Chem. Eng. J 354, 1083 (2018). doi:10.1016/j.cej.2018.08.035.

[16] S. Salvestrini, J. Jovanović and B. Adnadjević, Water Treat 57, 22868 (2016). doi:10.1080/ 19443994.2016.1180484.

[17] M. Zbair, A. El Hadrami, A. Bellarbi, M. Monkade, A. Zradba and R. Brahmi, JECE 8 (2), 103667 (2020). doi:10.1016/j.jece.2020.103667.

[18] S.K. Deokar, G.S. Bajad, P. Bhonde, R.P. Vijayakumar and S.A. Mandavgane, Waste J. Polym. Environ 25, 165 (2017). doi:10.1007/s10924-016-0794-3.

[19] J. Madejova, Vib. Spectrosc 31 (1), 1 (2003). doi:10.1016/S0924-2031(02)00065-6.

[20] F. Ayaria, E. Srasrab and M. Trabelsi-Ayadia, Desalin 185, 391 (2005). doi:10.1016/J. DESAL.2005.04.046.

[21] M.T. Wandembruck, A.T.A. Baptista, A.M. Vieira, D. Mantovani, J.F. Honorio, M.F. Vieira and R. Bergamasco, Engevista 20 (5), 732 (2018). http://periodicos.uff.br/. . ./15992

[22] A.M. Abdel–Aty, T.A. Gad-Allah, M.E. Ali and H.H. Abdel-Ghafar, Environ. Prog. Sustainable Energy 34 (2), 504 (2015). doi:10.1002/ep.12027.

[23] F.M. De Souza and O.A.A. Dos Santos, Environ. Technol 41 (5), 603 (2018). doi:10.1080/ 09593330.2018.1505967.